



# **iJRASET**

International Journal For Research in  
Applied Science and Engineering Technology



---

# **INTERNATIONAL JOURNAL FOR RESEARCH**

IN APPLIED SCIENCE & ENGINEERING TECHNOLOGY

---

**Volume: 11    Issue: VI    Month of publication: June 2023**

**DOI: <https://doi.org/10.22214/ijraset.2023.53989>**

**[www.ijraset.com](http://www.ijraset.com)**

**Call:  08813907089**

**E-mail ID: [ijraset@gmail.com](mailto:ijraset@gmail.com)**

# Amplitude Based Pilot Protection for Transmission Line

Amruta Narendra Wagh<sup>1</sup>, Ravindra. K. Munje<sup>2</sup>, Abhishek Srivastava<sup>3</sup>, Mohan P. Thakre<sup>4</sup>

Department of Electrical Engineering, K.K. Wagh Institute of Engineering Education and Research, Nashik, Maharashtra, India

**Abstract:** Distance protection and differential protection schemes are the two primary types of protection schemes employed in gearbox line protection today. However, industrial practice has shown that commonly used gap prevention techniques are limited in tripping speed and selectivity. The timing of the samples in each of the two relays located at the gearbox line terminals also affects the differential protection mechanism. On the other hand, pilot safety schemes using only the communication link to exchange local decision-making about fault conditions are not affected. These methods include protection of Extra High Voltage (EHV) and Ultra High Voltage (UHV) transmission lines. Synchronization of time. The problem of creating a fast and accurate fault detection system for the safety of EHV/UHV transmission lines, which is crucial in present power systems, is the subject of this master's thesis. The protection method described in this thesis is the foundation for the detection and analysis of waves travelling wave along transmission at fault initiation. This method compares the arrival of the first traveling waves at both ends of the protected line with respect to direction. This will establish whether the fault is located in the safe zone or not. Based on high voltage transmission network safety requirements a suitable phase sequence algorithm is developed to control single phase tripping. Finally, through simulations conducted in the MATLAB environment, practical design concerns for incorporating the newly proposed protection algorithm into a numerical relay unit are investigated.

**Keywords:** Transmission line protection, UHV relaying, traveling wave and numerical relay are other related terms.

## I. INTRODUCTION

The producing unit, transmission unit, and distribution unit are the three main units that make up an electric power system. In such a system, the transmission units are primarily in charge of delivering the generated electricity to the distribution units, which are situated near the major electric users. The performance of the gearbox unit is crucial since the goal of electric systems is to distribute electric energy to users. In a typical transmission unit, the transmission lines are used to carry electric energy over large distances. Transmission lines may take the shape of cables, overhead lines, or a combination of both. Because of their working environment, overhead lines are among them more vulnerable to errors. Lightning, conductor breakage due to thick ice coatings, or strong swings during stormy circumstances are some of the factors that might result in flashovers between conductors, to the ground, or across insulators [1]. These flashovers, along with malfunctioning machinery and ageing issues, exceed the imperative need for an appropriate protection strategy for precise fault detection on gearbox lines. A common relaying decision must almost always be made by relays positioned at terminals in order for the typical protection methods applicable to UHV/EHV transmission lines to function properly. It should therefore, be obvious that the success of the integrated communication system in this protection strategy is vital. This reliance on high performance communication systems has a greater impact on protection methods when relays are transferring power system phasor values. Conventional line differential and phase comparison protection techniques are two examples of such plans. To enable potential time synchronization between the two terminals, such methods should precisely time tag the instantaneous phasor data taken at predetermined moments in time. Since phasor data from both ends of protected line must be compared at the same location, a failure of synchronization between the relays could seriously impede the ability to detect problems. A defect on the protected line would be perceived as differences in the asynchronized phasor data at either end, which would cause the protection system to operate incorrectly. In today's differential protection schemes, some wrong operations resulting from synchronization failure brought on by communication channel asymmetry have been seen globally, as mentioned. The protection engineers occasionally use a different protection approach when there is a difficulty with the sharing of phasor data. In this approach, the initial fault detection is collected locally, and only the detected fault's state is relayed to the remote End relay across the communication channel. Conventional distance or directional comparison protection techniques use this type of relay for example.

Conventional protection strategies typically rely on monitoring the fundamental frequency components of power quantities, with the possible exception of any restrictions brought about by the inevitable use of communications in UHV/EHV transmission line protection. Consequently, a specific reliability decision is made after observing measurable components over a reasonable period of time. The period is often not one power frequency operating cycle. In the meanwhile, fault current can affect system stability and dramatically damage any equipment that is unable to sustain high fault current levels. Significantly faster fault detection for the system is made possible by protection strategies that exploit the traveling wave phenomenon on transmission lines. System acceleration can be restricted by the use of so-called ultra-high-speed (UHS) relays to protect critical transmission lines in the network. The generated rotational kinetic energy of the power system, this causes the system to accelerate and is inversely proportional to the square of the fault clearance time.

#### A. Transmission Line Protection

A power system is a sophisticated network with the primary responsibility of supplying electrical energy to network customers in a reliable manner. Power systems also have dynamic features that maintain a balance between the system's electricity production and consumption. Prior stick out to a new steady state operating condition, it may suffer transient instability conditions. Typical designs for such system components include fixed marginal operating boundaries and normal operating conditions as well as transient instability conditions. However, any malfunction of one or more pieces of equipment can cause anomalous behavior of the system. These unusual circumstances have the potential to seriously damage the machinery. Monitoring the performance of individual components and creating a safety strategy for the entire system is crucial to prevent serious damage and maintain normal operating conditions. Various protection schemes, often referred to as protection zones, are responsible for protecting electrical equipment located in defined overlapping zones while also providing protection for the overall system.

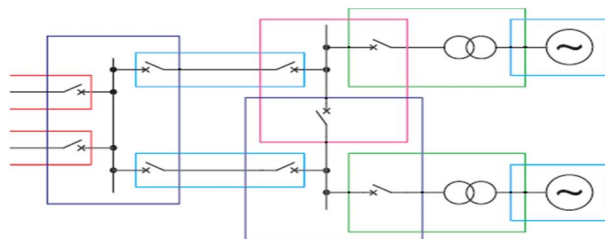


Fig. Protection Zones in A Power System

#### B. Traveling Waves on Transmission Lines

##### 1) Waves Traveling on Transmission Lines

According to studies on transients in power systems, the system experiences two primary categories of transients associated with electromechanical and electromagnetic phenomena, as shown in Fig. 2 is shown. The first results from the interaction of electrical energy stored in circuits and mechanical energy stored in the rotating machinery, a gang of vagrants .Different forms of transients are produced by the inter [14].

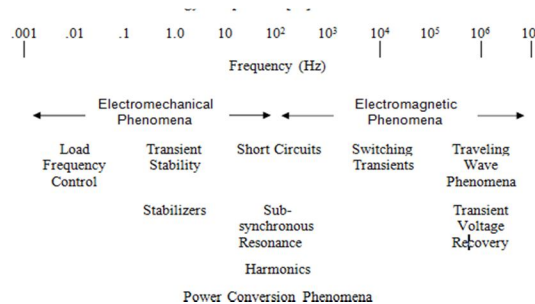


Fig.2Classifications of Power System several frequency tem Transients

A complicated power system has many ways and could show up as transient sources at several frequency band widths. Tansients propagate across a wide frequency spectrum, including DC, power frequency, and high frequencies, as a result of defects in transmission lines, which are one of the main causes of so called travelling wave phenomenon.

## II. LITERATURE REVIEW

To reduce dependence on fossil fuels, modern power systems have made significant use of renewable energy sources (RESs) [1-2]. RES is usually integrated through the power plant's collector system and connected to nearby local substations to reduce costs [3-4]. It is important to ensure that the gearbox line protection system is functioning properly because any failure or malfunction will seriously threaten the stability of the power system and the safety of the power equipment [5].

Inverter-interface renewable energy generators (IIREGs), also known as photovoltaic (PV) and permanent magnet synchronous generators (PMSGs), have grown rapidly in recent years [6]. A power inverter is used to integrate the IIREG with a synchronous grid [7]. A fault current limiter (FCL) is equipped at the output of the inverter to protect these devices because the inverter has a poor ability to withstand overcurrent [8-9]. Alternatively, control system based current limiters are employed. IIREGs have very different fault behavior from synchronous generators (SGs), which mainly exhibit limited current amplitude, unstable system impedance and controlled current phase angle [10-11]. These fault behaviors are influenced by the control techniques of the FCL and the inverter.

For internal failures, differential protection should be activated in a matter of tens of milliseconds. A controlled phase angle, however, will result in a failure of the proportional brake differential protection. It has been found that the current phase difference will be high and this can be greater than  $90^\circ$  for phase-to-phase faults when the short-circuit capacity for IIREGs is equal to a quarter of the synchronous grid [16]. This will affect the proper operation of differential protection. Furthermore, when the fault current from the IIREGs was significantly smaller than the grid fault current, the operating current magnitude approached the restraint current. This situation will also lead to a reduction in the sensitivity of the proportional brake differential protection [17]. To address the above issues, several innovative conservation strategies have been put forward. Literature [18] describes how to construct equivalent differential impedance using differential voltage and current and how to use the amplitude characteristics of the differential impedance to differentiate between internal and external faults. However, this method has strict requirements for synchronous data transmission. Reference [19] constructs differential protection using differential magnitude characteristics and breaking impedances, although it may not work if there is fault resistance. Parameter identification as a form of protection was introduced in [20-21].

This approach is based on the distinction between whether the time-domain differential is a first-order derivative

The voltage and differential current satisfy the capacitance model [21], but the first derivative is significantly affected by higher harmonics, requiring improved performance. A traveling-wave-based pilot protection was put forward by the authors in [22, 23], although it is more sensitive to **transients** and requires a higher sampling frequency.

In addition, the similarity index between the transient currents at both ends was calculated using Pearson correlation coefficient and cosine similarity, but it will not work when the IIREGs produce low power due to insufficient light or wind or the current breaker is re-closed with permanent failure.

## III. PROPOSED SYSTEM

### A. Simulation Model for Study of Transients on Transmission Line

The power system model shown in Fig. 3 was created using the frequency dependent transmission line model offered in MATLAB was used to generate the power system model.

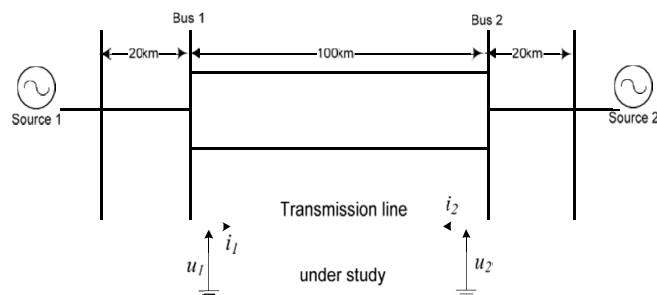


Fig.3 Power system used for simulations

This models transmission line is parallel to another transmission line that runs between buses 1 and 2 and has a length of 100km and voltage level of 230kV. The load current in this system is produced by adding a 20-degree phase variation between two 140-km-apart voltage sources. Additionally, labeled voltage and current signal values are saved for later examination. With the help of this model, we can examine the characteristics of traveling wave reflection and refraction. Discontinuities are introduced at the bus bars and sources sites when travelling waves run into various characteristic impedances.

The simulation results of the voltage and current signals recorded on Bus 1, the location of the phase-A-to-ground fault in the middle of the transmission line, are shown in Figure 4. The fault is applied at  $t=0.202794$ s and the simulation lasts 0.3 s. lasts until For brief periods, less than one cycle of the power system frequency, high frequency variations in voltage, and current signals due to reflections of traveling waves in the system can be seen in both measured signals. A detailed look at the high frequency fluctuations shown in Figure 4 is shown in Figure 5. the initial deviation in the voltage and current signals at time T1 indicates the arrival of traveling waves that travel 50 kilometers (km) in less than 0.16 milliseconds from the midpoint of the transmission line to bus 1. The traveling waves first encounter a discontinuity at bus 1, where they are reflected and refracted as previously mentioned. the distance. There is 40 kilometers between bus 1 and the nearest discontinuity (which is at source 1), but the reflected wave must travel 100 kilometers to reach fault point F before return.

1. The first and second traveling waves reflected from the position of source 1 are therefore indicated by the deviations in the voltage and current signals appearing at  $t_2$  and  $t_3$  respectively, while the deviations at  $t_4$  indicate the second traveling waves reflected from the fault site F. In addition, the first deviation in the recorded signals has a maximum amplitude, and subsequent deviations have lower amplitudes due to the decreasing energy of the reflected traveling waves. In addition, Fig. As shown in Figure 4, the traveling wave reflects itself until it runs out of energy and ceases to exist. Finally, the deflections at  $t_1$  and  $t_4$  in Figure 5 show that the traveling waves reflected from the fault point have the same polarity at all times. On the other hand, the polarity of the returning waves will change if they are reflected from different places.

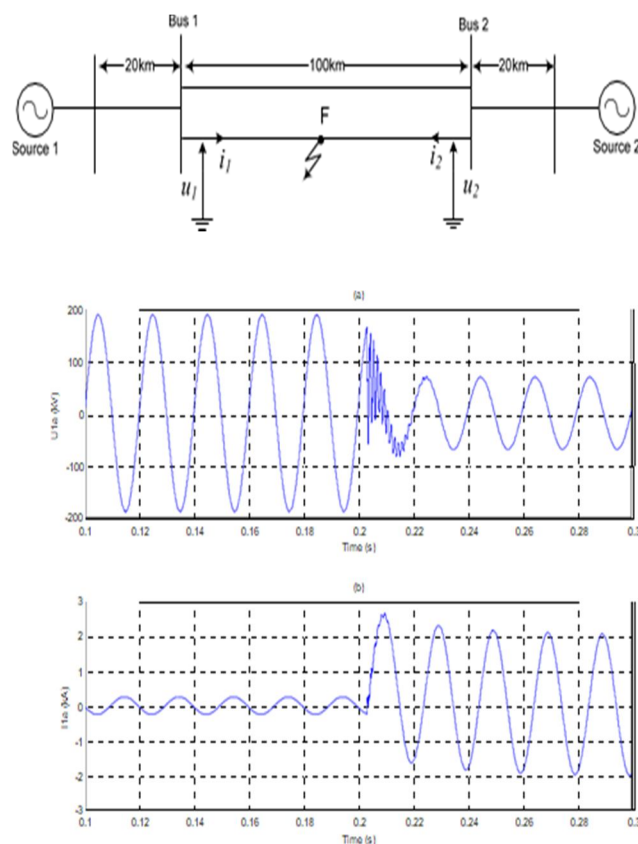


Fig. 4 Power Quantities Measured At The Transmission Line's Midway At The Beginning Of The Phase-A-To-Ground Fault; (A) Phase Voltage Signal Measured At Bus1;(B) Phase Current Signal Measured At Bus1.

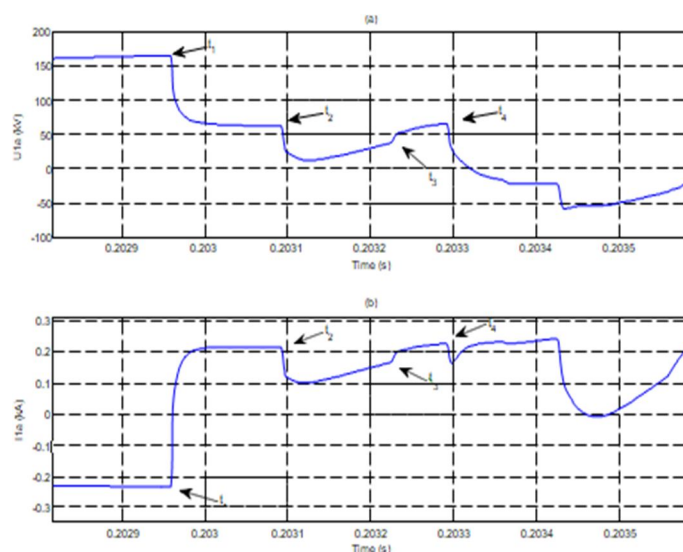


Fig. 5 Close-up of changes in measured power values caused by the occurrence of a phase-a-to-ground fault at the transmission line's mid-way and there flection of travelling waves in the system; (a) measured phase voltageat Bus1; (b) measured phase current at Bus1.

### B. Proven Issues with Actual Implementation

Recent proposals for digital relays call for converting continuous data sequences in analog signals to profane data before switching from analog to digital technology. These data are samples obtained at predetermined time intervals from the original analog signals. Consequently, the Nyquist frequency, which is the highest frequency present in digital signals, has a finite range and is highly influenced by the sampling rate. In order to convert analogue signals, non-bounded frequency analogue signals must be constrained to bounded frequency signals. Due to the much higher rate of change of the analog signal than the sampling rate, this condition is necessary to prevent the conversion from naming another signal instead of the original analog signal. Therefore, before sampling, frequencies outside the Nyquist bandwidth must be excluded. A low pass filter having a cut-off frequency of  $f_c$  is shown in Fig. 6 with a typical frequency response. When an analog signal is used as the input signal of a filter, an LPF known as an anti-aliasing filter can produce satisfactory attenuation of the frequency components at  $f_c$  (equivalent to the Nyquist frequency). Consequently, the output signal from such filtering is an analog signal with a more or less band-limited frequency that can be used for further sampling. It should be noted that anti-aliasing filters allow some aliasing to occur due to the imperfect LPF characteristic, resulting in attenuation rather than complete rejection of high frequency components. The needs of signal processing should be met by this. To sample analogue signals at a very high sampling frequency is one of the realistic solutions to this problem. To sample analogue signals at a very high sampling frequency is one of the realistic solutions to this problem. This method is often used in digital signal processing and is known as the oversampling approach. The needs of signal processing should be met by this. To sample analogue signals at a very high sampling frequency is one of the realistic solutions to this problem.

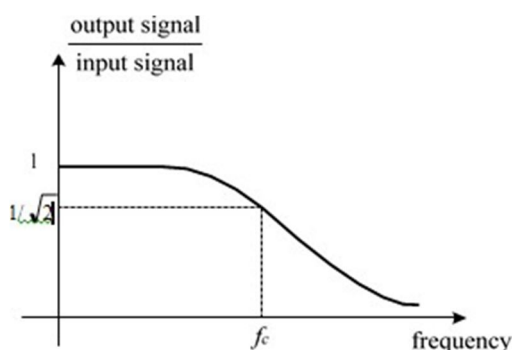


Fig.6ConventionalLowPassFilterFrequencyResponse

Anti-aliasing filters are designed to reject high frequency components that are considered noise in standard protection algorithms based on fundamental frequencies. The sharp cut-off frequencies of these anti-aliasing filters add some processing time to the signal. However, anti-aliasing filters with high cut-off frequencies are frequently utilised in proposed travelling wave relays to reflect the wide frequency components of unbounded analogue signals into a bounded frequency digital signal. This reduces the delay introduced by the filtering process. The presence of other high frequency components in the measured signal (potential interference signals) makes it.

It is difficult to choose high cut-off frequencies, on the order of MHz. These additional components are considered noise because they represent sudden amplitude shifts between digital samples. Fig. 7 shows the presence of a short period of white noise on the voltage signal recorded at the beginning of the simulation. White noise can be identified as traveling waves that may or may not be present in the system and appear as high frequency transients in the measured signal. Accordingly, abrupt changes in the amplitude of the observed voltage and current waveforms relative to their steady state values are not sufficient criteria to identify transients associated with traveling waves. This problem highlights the need to develop algorithms with additional criteria to distinguish high frequency transients from fault induced transients, which may have a different source. Various traveling wave detection techniques have been described in the literature to extract high frequency transients when noise is present in recorded signals. Reliable traveling wave detection has been addressed using various techniques such as integrating time-frequency domain signal processing methods. The development of traveling wave detection techniques in this situation usually complicates the overall protection strategy and requires the use of large, high-performance processors to integrate the techniques into numerical relays.

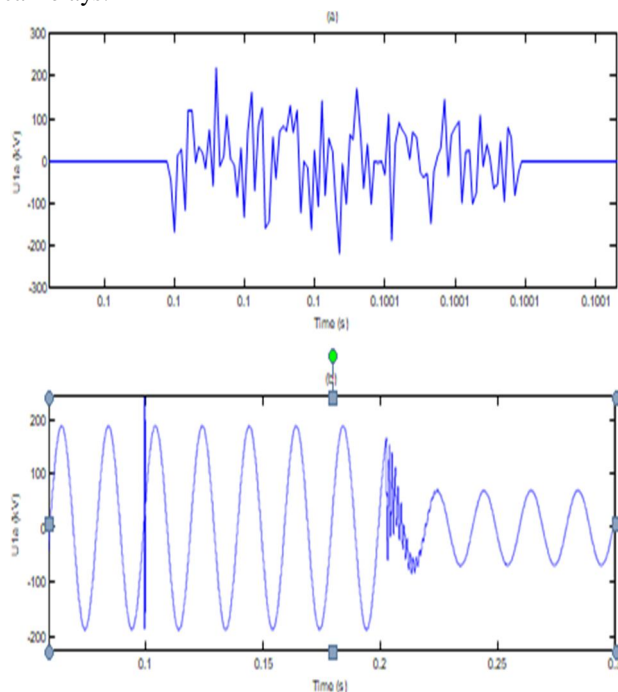


Fig.7 With noise transients (a) high frequency noise transients (b) high frequency noise transients followed by high frequency travelling wave transients are seen in the measured voltage signal at the onset of a single-phase fault internal to the measurement site.

The requirement for model transformation of three-phase power system components adds another challenge to the implementation of such designs. The three phase voltage signals produced by simulating a single-phase-to-ground fault are shown in Figure 8. Cross coupling between the three phase's results in high frequency transients on the 'healthy' phases B and C. A traveling wave propagating over a faulty phase A. For measured signals associated with healthy phases, this sounds like transient noise.

It is usually necessary to work with modal voltage and current components instead of phase components in the proposed strategy based on traveling waves to arrive at the correct conclusions. In addition, fault detection algorithms should offer phase selectivity because it is undesirable for a transmission line to trip three phases for a single-phase failure. This increases the complexity of such protection strategies and calls for the use of additional algorithms for phase selections based on modal analysis.

### C. Envisioned Protection Plan

This section explains the decision-making process in the proposed transient-based protection system as well as the general operation of the numerical relay model employed in the scheme. A model for a transient-based numerical relay unit placed at each terminal of a transmission line is shown in Fig. 10 is indicated using the pilot protection scheme diagram shown in Figure 9.

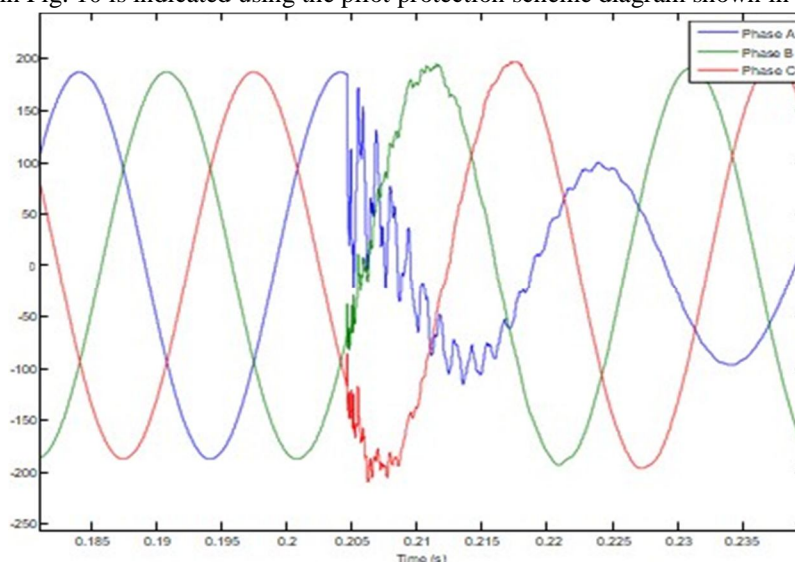


Fig. 8 When a single-phase fault develops internally to the measurement site, the effect of mutual coupling in three phase recorded voltage signals is seen.

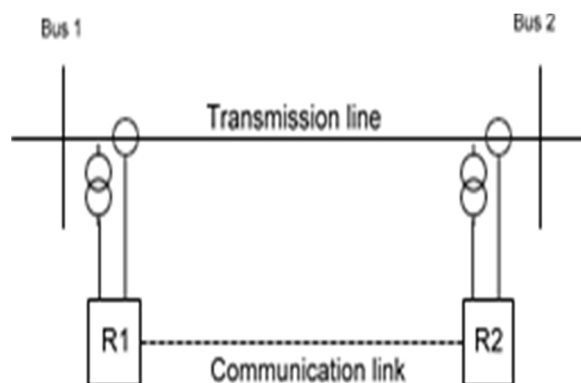


Fig.9 Pilot Protection System For Transmission Line Single Line Diagram

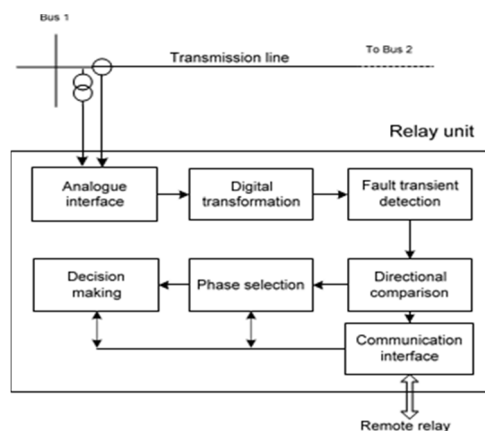


Fig. 10Unit with A Transient-Based Numerical Relay

In such a relay unit, the analog interface unit, which is shown in Fig. 10, where data processing of the signals begins. The protection strategy is based on comparing the polarity of fault transients in the voltage and current signals, therefore the analogue interface unit accepts analogue readings of three-phase current and voltage from the secondary side of the measuring equipment. After that, an analogue to digital converter processes the signals. Digital Transformation Unit. Consequently, the input of the fault transient detection unit will be able to accept the converted digital voltage and current. Polarity of fault transients in the voltage and current signals. The signals are then passed through an analog to digital converter. Digital Transformation Unit. Consequently, the input of the fault transient detection unit will be able to accept the converted digital voltage and current. Indications. Fig. 3.9 illustrates the progressive measurement and digital conversion of analogue voltage and current data for a faulty phase at one end of a transmission line. The voltage signal that was measured on the CCVT's secondary side is distorted, representation of the voltage signal actually present on the primary side of the device. However, this approach uses the low frequency components of the observed signals during the analog to digital conversion process using a second order Butterworth LPF with a cut-off frequency of 1 kHz. In addition, Fig. As shown in 3.9, the attenuation introduced by low pass filtering does not significantly affect the analysis of transients at low frequencies because the primary changes in the amplitude of the monitored signals then occur over a wide range of frequencies. Doshia arises. As a result, after passing through the transformation unit, a digital voltage signal is obtained that contains frequency components suitable for further transient analysis. The observed current signals pass through the same analog to digital conversion as shown in Fig. appears in 11. A band stop

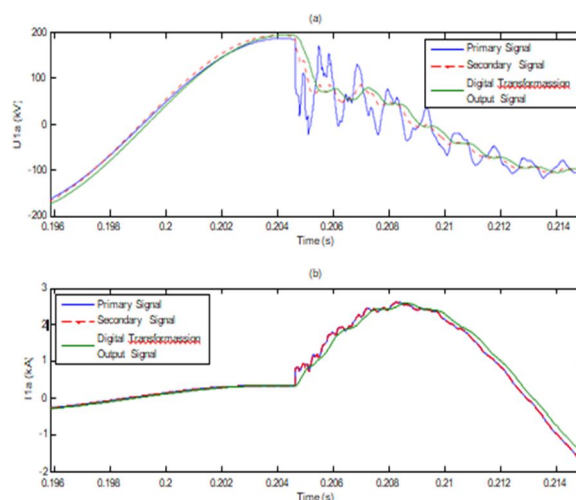


Fig. 11 Signals for starting a single-phase fault inside the measuring point that are converted from analogue to digital are (a) voltage signals and (b) current signals.

filter (BSF) is used in fault transient detection units as a practical way to remove high frequency transients applied to steady state signals. BSF has the ability to narrow down a certain bandwidth of frequencies. Therefore, the superimposed transients at the onset of the fault are extracted by using this steady state suppressor and rejecting the steady state frequency components.

#### IV. CURRENT AMPLITUDE COMPARISON BASED PILOT PROTECTION

##### A. Basic Principle

All IIREGs are connected to collector lines, and the generated power is carried through transmission lines. Due to the high voltage level, the main transformers on both sides of the line are grounded.  $E_P$  and  $E_Q$  represent the equivalent IIREG and grid internal potential, respectively.  $U_f$  is the residual voltage at the fault location due to the fault resistance.  $Z_P$  and  $Z_Q$  represent the equivalent IIREG and grid internal impedances, and  $Z_L$  is the sum of the impedances of the entire outgoing transmission line. Further,  $\lambda$  represents the ratio of line impedance to  $Z_L$  between the fault location on the grid side and the bus bar and ranges from 0 to 1. For the fault model of IIREGs,  $E_P$  is assumed equal to  $E_Q$ , and the fault current of IIREGs is simulated by adjusting the equivalent impedance  $Z_P$ . This means that the  $Z_P$  varies for different fault locations. Although RES is equivalent to a controlled current source in many respects that may better reflect its fault characteristics, the equivalent manner of a voltage source and large impedance has the same effect.

In this case, the fault currents can be written as:

$$I_P = \frac{E_P - U_F}{Z_P + (1-\lambda)Z_L} \quad (1)$$

$$I_Q = \frac{E_Q - U_F}{Z_Q + \lambda Z_L} \quad (2)$$

Since  $E_P$  is considered to be equal to  $E_Q$ , the current amplitude ratio is expressed as:

$$\left| \frac{I_P}{I_Q} \right| = \frac{Z_Q + \lambda Z_L}{Z_P + (1-\lambda)Z_L} \quad (3)$$

Normally, the fault current from IIREGs is below twice the nominal current due to the effect of FCLs. Therefore,  $Z_P$  is usually much larger than  $Z_Q$ . Consequently, the numerator in Eq. (3) is less than the denominator and the ratio is usually smaller than 1, so the conservation criterion is given by:

$$\xi = \left| \frac{I_P}{I_Q} \right| < P_{set} \quad (4)$$

where  $|\cdot|$  i.e. the amplitude of a particular phasor. Furthermore,  $P_{set}$  represents the threshold of the proposed criterion. The amount of RES will be increased in future. In some areas, short-circuits from IIREGs can contact power connected systems. In this case, the basis that  $|Z_P| > |Z_Q|$  larger than will not establish for long and the protection will refuse to function. Therefore, this criterion must have a specific scope of application. To calculate the length limit, the scenario that is most likely to fail (a fault located at bus P,  $\lambda=1$ ) is analyzed, and (3) is simplified as:

$$\xi = \frac{|Z_Q + Z_L|}{|Z_P + Z_L|} \approx \frac{|Z_Q| + |Z_L|}{|Z_P| + |Z_L|} < P_{set} \quad (5)$$

$$|Z_P| > |Z_P|$$

When the IIREG short-circuit capability reaches  $1/\beta$  of the connected grid,  $Z_P$  can be considered equal to  $\beta Z_Q$ . Further, the fault current provided by IIREGs is taken as maximum  $2I_N$ . Based on this, the minimum IIREG internal impedance can be calculated as:

$$Z_{P,min} = \frac{E_P}{2\sqrt{3}I_N} \quad (6)$$

## V. THE PERFORMANCE UNDER DIFFERENT SCENARIOS

### A. Operating Performance for Teed Lines

Operating performance when the breaker is reclosed

To deal with the low sensitivity or rejection of traditional differential protection, some scholars propose new pilot protection principles using the difference in transient current waveforms at both ends. Pearson correlation coefficient and cosine similarity can be used to measure this feature, and both equations are as follows:

$$\left\{ \begin{array}{l} \text{pearson}(x, y) = \frac{\sum_{i=1}^n \left( X_i - \frac{1}{n} \sum_{j=1}^n X_j \right) \left( Y_i - \frac{1}{n} \sum_{j=1}^n Y_j \right)}{\sqrt{\sum_{i=1}^n \left( X_i - \frac{1}{n} \sum_{j=1}^n X_j \right)^2} \sqrt{\sum_{i=1}^n \left( Y_i - \frac{1}{n} \sum_{j=1}^n Y_j \right)^2}} \\ \text{Cos}(x, y) = \frac{\sum_{i=1}^n (X_i \cdot Y_i)}{\sqrt{\sum_{i=1}^n X_i^2} \sqrt{\sum_{i=1}^n Y_i^2}} \end{array} \right. \quad (7)$$

where Pearson (x, y) and cos(x, y) are two current waveforms with  $y=[y_1, y_2, \dots, y_n]$ , Pearson correlation coefficient and cosine similarity of  $x=[x_1, x_2, \dots, x_n]$  is. Furthermore, two coefficients range from -1 to 1.

With the addition of plant 2 the flow on the P side will be less than that on the Q side. As the capacity of Plant 2 increases, the protection may fail. During normal operation, the current phase of plant 1 is substantially the same as that of plant 2, so the protection fault occurs when the rated capacity of plant 2 theoretically reaches 18% of that of plant 1 due to a setting value of 0.82. . Therefore, the criteria must be revised. After plant 2 is connected, during normal operation the current relationship satisfies:

$$I_P + I_W = -I_Q \quad (1)$$

At this point,  $I_P + I_W$  includes phase or transmission, which increases the communication pressure. To reduce the need for communication, the criteria are considered to be rewritten as:

$$\xi = \frac{|I_P| + |I_W|}{|I_Q|} \leq \frac{P_{set}(2)}{|I_Q|}$$

First, the performance of (2) for external faults is analyzed. According to the properties of the absolute value inequality, (3) is obtained

$$|I_P + I_W| = |I_Q| \leq |I_P| + |I_W| \quad (3)$$

Therefore, the expression of the value  $\xi$  is given:

$$\xi = \frac{|I_P| + |I_W|}{|I_Q|} \geq 1 \quad (4)$$

It can be seen from (4) that the improved criterion will not cause a fault when the system operates normally or when an external fault occurs at F4. Furthermore, for external faults at point F, the phasor relation is satisfied as:

$$I_W + I_Q = -I_P \quad (5)$$

$$|I_W + I_Q| \geq |I_Q| - |I_W| \quad (6)$$

Combining (5) and (6), the value  $\xi$  could be written as:

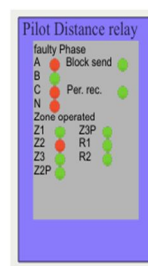
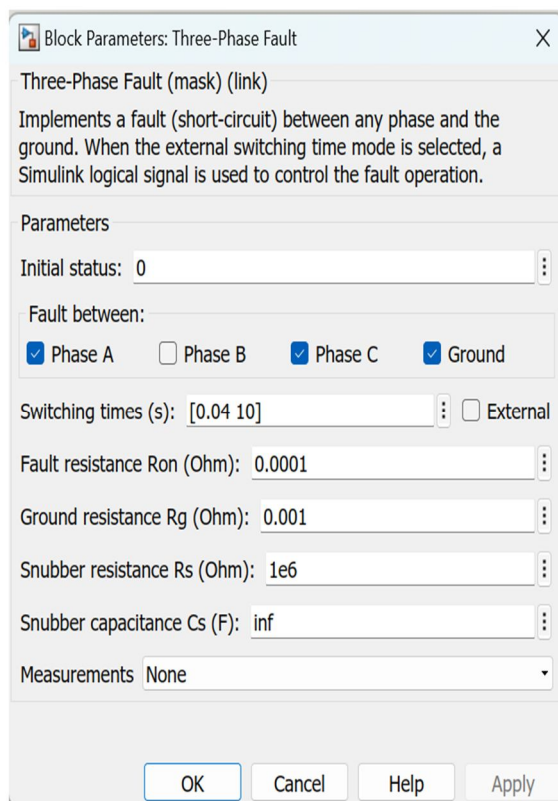
$$\xi = \frac{|I_P| + |I_W|}{|I_Q|} \geq 1 \quad (7)$$

It is clear from (7) that the defense will also not be defective. Similarly, it can also be proved that the protection will not be defective for external faults at other locations. The equivalent fault for an internal fault at F1.ZL1 and ZL2 are the positive-sequence impedances of lines L1 and L2 respectively,  $\lambda_1$  can be calculated using the line impedance between the fault location and point O divided by ZL1 and ZW.  $\Sigma$  is the sum of the internal impedance ZW of plant 2 and the impedance ZL3 of line L3. It is clear that the grid-side fault current can be calculated as:

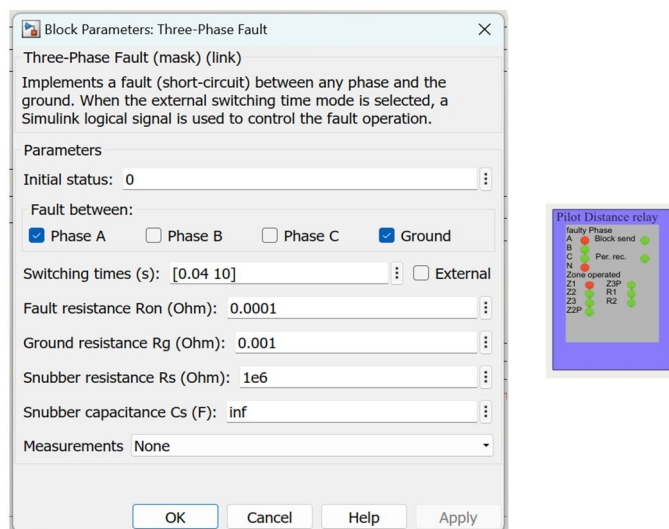
$$\dot{I}_Q = \frac{\dot{E}_Q - \dot{U}_f}{(Z_{12} + Z_Q + \lambda_1 Z_{L1}) \left( 1 + \frac{\lambda_1 Z_{L1} (Z_{12} + Z_Q)}{Z_{W\Sigma} (Z_{12} + Z_Q + \lambda_1 Z_{L1})} \right)} \quad (8)$$

In (8), since  $\lambda_1 Z_{L1}$  is only a small part of the transmission line, it must be much smaller than  $Z_{W\Sigma}$ . On the other hand,  $Z_{L2} + Z_Q$  is smaller than  $Z_{L2} + Z_Q + \lambda_1 Z_{L1}$ . Therefore, the denominator is approximately equal to  $Z_{L2} + Z_Q + \lambda_1 Z_{L1}$ , and the W branch has little effect on the grid-side phase current.

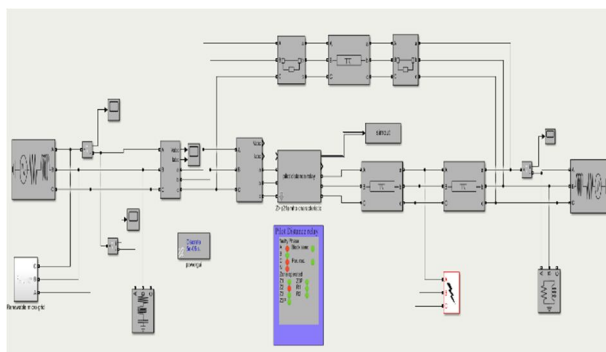
## VI. RESULTS



Result 1: Fault\_introduced\_with\_result



Result 2: Fault introduced with result



Simulation

## VII. CONCLUSION

The following conclusions are drawn after researching how the travelling wave concept can be used to develop new transmission line protection algorithms : The analysis of the practical implementation of the travelling wave idea in the development of startups uses the research of the travelling wave concept in transmission lines. UHS Conservation Program. This paper examines the potential challenges in creating such schemes due to the absence of the necessary hardware technology in recent years. Recent approaches to the installation of traveling wave relays using contemporary technology are analyzed. Where two categories of barriers to the implementation of these systems in practice are mentioned. Special requirements in signal measurement. And data processing is detected by checking valid limits. The creation of travelling wave protection methods can be made simpler using an effective method that is based on the analysis of fault-induced transients at band-limited frequencies. The restricted frequency response of the measuring equipment used in this technique has no effect on the fault finding process. Additionally, labor-intensive digital data processing is no longer required. Because of these successes, the solution is now likely to be implemented in existing digital relay platforms With phase selection capabilities that can differentiate between the phases involved in fault start, the protection algorithm created for this system offers directional fault detection. A review of the simulation results shows that the suggested protection strategy is able to accurately detect faults in the protection zone and remains protected for faults outside the protection zone. Additionally, this scheme has a UHS decision-making process for faults that enables fast and targeted fault detection. Consequently, the proposed transmission line protection scheme solves a number of problems using established transmission line protection schemes. Furthermore, this technique can be successfully implemented in standard numerical relay units without many difficulties or unique requirements, unlike previous traveling wave schemes.

## REFERENCES

- [1] M. B. Mcelroy and X. Chen, "Wind and solar power in the united states: status and prospects," in CSEE Journal of Power and Energy Systems, vol. 3, no. 1, pp. 1-6, March 2017.
- [2] W. Du, J. Bi, T. Wang and H. Wang, "Impact of grid connection of large scale wind farms on power system small-signal angular stability," in CSEE Journal of Power and Energy Systems, vol. 1, no. 2, pp. 83-89, June 2015.
- [3] V. Miranda, "Successful large-scale renewables integration in Portugal: Technology and intelligent tools," in CSEE Journal of Power and Energy Systems, vol. 3, no. 1, pp. 7-16, March 2017.
- [4] A. Prasai, J. Yim, D. Divan, A. Bendre and S. Sul, "A New Architecture for Off shore Wind Farms," in IEEE Trans. Power Electron., vol. 23, no. 3, pp. 1198-1204, May 2008.
- [5] J. He, Z. Wang, Q. Zhang, L. Liu, D. Zhang and P. A. Crossley, "Distributed protection for smart substations based on multiple overlapping units," in CSEE Journal of Power and Energy Systems, vol. 2, no. 4, pp. 44-50, December 2016.
- [6] Z. Chen, X. Pei, M. Yang, et al, "A Novel Protection Scheme for Inverter-Interfaced Microgrid (IIM) Operated in Islanded Mode," in IEEE Trans. Power Electron., vol. 33, no. 9, pp. 7684-7697, Sept. 2018.
- [7] B. Liu, Q. Wei, C. Zou and S. Duan, "Stability Analysis of LCL-Type Grid-Connected Inverter Under Single-Loop Inverter-Side Current Control With Capacitor Voltage Feedforward," in IEEE Trans. Ind. Informat., vol. 14, no. 2, pp. 691-702, Feb. 2018.
- [8] H. Nourmohamadi, M. Sabahi, E. Babaei and M. Abapour, "A New Structure of Fault Current Limiter Based on the System Impedance With Fast Eliminating Method and Simple Control Procedure," in IEEE Trans. Ind. Electron., vol. 65, no. 1, pp. 261-269, Jan. 2018.
- [9] H. A. Pereira, R. M. Domingos, L. S. Xavier, A. F. Cupertino, V. F. Mendes and J. O. S. Paulino, "Adaptive saturation for a multifunctional three-phase photovoltaic inverter," 2015 17<sup>th</sup> European Conference on Power Electronics and Applications (EPE'15 ECCE-Europe), Geneva, 2015, pp. 1-10.
- [10] L. Chen and S. Mei, "An integrated control and protection system for photovoltaic micro grids," in CSEE Journal of Power and Energy Systems, vol. 1, no. 1, pp. 36-42, March 2015.
- [11] R. Tao, F. Li, W. Chen, et al, "Research on the protection coordination of permanent magnet synchronous generator based wind farms with low voltage ride through capability," in Protection and Control of Modern Power System, vol. 2, no. 3, pp. 311-319, July 2017.
- [12] K. Jia, C. Gu, Z. Xuan, L. Li and Y. Lin, "Fault Characteristics Analysis and Line Protection Design Within a Large-Scale Photovoltaic Power Plant," in IEEE Trans. Smart Grid, vol. 9, no. 5, pp. 4099-4108, Sept. 2018.
- [13] A. Hooshyar and R. Iravani, "A New Directional Element for Microgrid Protection," in IEEE Trans. Smart Grid, vol. 9, no. 6, pp. 6862-6876, Nov. 2018.
- [14] V. Telukunta, J. Pradhan, A. Agrawal, M. Singh and S. G. Srivani, "Protection challenges under bulk penetration of renewable energy resources in power systems: A review," in CSEE Journal of Power and Energy Systems, vol. 3, no. 4, pp. 365-379, Dec. 2017.
- [15] J. He, L. Liu, F. Ding, et al, "A new coordinated backup protection scheme for distribution network containing distributed generation," in Protection and Control of Modern Power System, vol. 2, no. 1, pp. 102-110, Mar. 2017.
- [16] Y. Li, K. Jia, T. Bi, et al, "Analysis of line current differential protection considering inverter-interfaced renewable energy power plants," 2017 IEEE PES Innovative Smart Grid Technologies Conference Europe (ISGT-Europe), Torino, 2017, pp. 1-6.
- [17] S. Dambhare, S. A. Soman and M. C. Chandorkar, "Adaptive Current Differential Protection Schemes for Transmission-Line Protection," in IEEE Trans. Power Del., vol. 24, no. 4, pp. 1832-1841, Oct. 2009.
- [18] T. G. Bolandi, H. Seyedi, S. M. Hashemi and P. S. Nezhad, "Impedance Differential Protection: A New Approach to Transmission-Line Pilot Protection," in IEEE Trans. Power Del., vol. 30, no. 6, pp. 2510-2518, Dec. 2015.
- [19] G. Chen, Y. Liu and Q. Yang, "An Impedance-based Protection Principle for Active Distribution Network," 2018 China International Conference on Electricity Distribution (CICED), Tianjin, 2018, pp. 1241-1245.
- [20] Xiaoning Kang, Jiale Suonan, Guobin Song and Z. Q. Bo, "Protection technique based on parameter identification its principle and application," 2008 IEEE Power and Energy Society General Meeting - Conversion and Delivery of Electrical Energy in the 21st Century, Pittsburgh, PA, 2008, pp. 1-6.
- [21] X. Kang, Z. Wu, J. Suonan and H. You, "Research on pilot differential protection based on parameter identification and suitable frequency band of transmission line model," 2011 International Conference on Advanced Power System Automation and Protection, Beijing, 2011, pp. 234-241.
- [22] F. V. Lopes, C. M. S. Ribeiro, J. P. G. Ribeiro and E. J. S. Leite, "Performance evaluation of the travelling wave-based differential protection when applied on Hybrid Transmission Lines," in The Journal of Engineering, vol. 2018, no. 15, pp. 1114-1119, 10 2018.
- [23] X. Dong, J. Wang, S. Shi, B. Wang, B. Dominik and M. Redefern, "Traveling wave based single-phase-to-ground protection method for power distribution system," in CSEE Journal of Power and Energy Systems, vol. 1, no. 2, pp. 75-82, June 2015.



10.22214/IJRASET



45.98



IMPACT FACTOR:  
7.129



IMPACT FACTOR:  
7.429



# INTERNATIONAL JOURNAL FOR RESEARCH

IN APPLIED SCIENCE & ENGINEERING TECHNOLOGY

Call : 08813907089  (24\*7 Support on Whatsapp)